Reversible Association of Thermoresponsive Gold Nanoparticles: Polyelectrolyte Effect on the Lower Critical Solution Temperature of Poly(vinyl methyl ether)

Rama Ranjan Bhattacharjee, Mukut Chakraborty,† and Tarun K. Mandal*

Polymer Science Unit, Indian Association for the Cultivation of Science, Jadavpur, Kolkata 700 032, India

Received: November 18, 2005; In Final Form: February 7, 2006

Thermoresponsive gold nanoparticles (GNPs) have been prepared by the borohydride reduction of gold salt in the presence of water-soluble polymer, poly(vinyl methyl ether) (PVME). The PVME-coated GNPs (PVME-GNPs) have been assembled into large aggregates in the presence of polyelectrolytes, viz., poly(sodium-4 styrene sulfonate) and sodium salt of carboxymethylcellulose at low pH by raising the solution temperature from 20 to 40 °C. Increase of temperature triggers the interparticle association due to hydrophobic interaction of pendent methyl group of the surface adsorbed PVME. This assembly process is reversible with respect to temperature and pH of the medium and was studied by monitoring the change in surface plasmon resonance band of PVME-GNPs. Three-dimensional assemblies of various architectures, depending on the concentration of polyelectrolytes, were observed through transmission electron microscopy. A mechanistic model has been suggested for the reversible assembly formation that suits well with the experimental observations. The changes in optical properties of the PVME-GNPs due to their aggregation/disaggregation enabled us to use it as an effective tool to monitor the change in lower critical solution temperature (LCST) of PVME in the presence of polyelectrolytes due to interpolymer complexation at low pH. This result agrees well with the variation of LCST of pure aqueous PVME solution in the presence of polyelectrolytes measured by conventional turbidimetric technique.

Introduction

Surface-modified nanoparticles are now a day used as versatile building blocks for preparing novel nano-structured materials and devices with the expectation that the collective physicochemical properties of assembled materials would be different from those of the isolated nanoparticles.[1−4] The obstacles faced to prepare those structural materials or to fabricate nanodevices are daunting, as one needs to have a good control on the size and shape of these nanoparticles and their assemblies. Thus, a major challenge in nanoparticles-based materials chemistry is the standardization of suitable methods to control the assemblies of these nanoparticles. To fill this growing need, several different strategies have been developed to assemble gold nanoparticles (GNPs) into ordered structural materials with unique properties. They include electrostatic interaction,[5] metal ion directed assembly,[6] DNA-driven assembly,[1] hydrogen bonding,[7,8] Langmuir−Blodgett technique,[9] cross-linking via bifunctional molecules,[10,11] block copolymer/surfactant mediated self-assembly,[12] protein-mediated particle assembly,[2,3] antigen−antibody interactions,[4] and biotin−avidin interactions.[2] The color as well as spectral changes induced by the assembly of nanometer-sized GNPs provide basis of a simple and highly selective method for the detection of biological molecules[4] and metal ions by anchoring ligand molecules specific for receptor molecules in the solution.[13] This technique has also been exploited to study the interfacial properties of peptides.[14]

Polymers or surfactant systems interacting with GNPs has been explored as a means for particle size control, stabilization to avoid aggregation, and formation of self-assembled materials.[5,8] GNPs stabilized with a hydrophilic polymer are especially important because of their compatibility with bio-analytical and biomedical requirements.[15−17] In general, polymers functionalized with thiol or amine groups capable of interacting with gold surface are used to prepare stable colloidal GNP suspensions.[18−20] Although, we have reported the synthesis of colloidal GNPs by the polymer in situ redox technique using poly(4-vinyl phenol) as a simultaneous template/stabilizer and reducing agent.[21] In this paper, we have synthesized colloidal GNPs by employing a water-soluble synthetic polymer, poly(vinyl methyl ether) (PVME) as a template/stabilizer. PVME, a well-known thermoresponsive polymer, is soluble in water below its lower critical solution temperature (LCST) at about 34 °C but forms macroscopic conservator phases due to hydrophobic interaction of pendent methyl group above that temperature.[22] This type of phase behavior is interesting to study as it has certain similarities with the denaturation of proteins as well as to temperature control mechanism in homoeothermic animal.[23] It has also been reported that the LCST of PVME is effected by polyacids such as poly(acrylic acid) (PAA) due to interpolymer complex (IPC) formation through successive H-bonding and/or hydrophobic interactions between PVME (polybase) and PAA.[24,25] Here, we have employed this phenomenon of interpolymer complexation to demonstrate reversible assembly of thermosensitive PVME-coated GNPs (PVME-GNPs) by introducing polyelectrolytes, viz., poly(sodium-4 styrene sulfonate) (PSS) and sodium salt of carboxymethylcellulose (NaCMC). The change in surface plasmon resonance (SPR) property of GNPs due to this assembly provided us the opportunity to study the phase behavior of aqueous PVME solution and to investigate the phenomenon of interpolymer complex formation. This spectroscopic method would be simpler

* To whom correspondence should be addressed. Fax: 91-33-2473 2805. E-mail: psutkm@mahendra.iacs.res.in.

† Present Address: Maharaja Manindra Chandra College, Kolkata-3, India.

10.1021/jp056675b CCC: $33.50
Published on Web 03/09/2006

and relatively more accurate than the earlier reported methods, used in the investigation of IPCs.[26−28]

Experimental Section

Materials. Hydrogen tetrachloroaurate trihydrate ($HAuCl_4 \cdot 3H_2O$) and sodium borohydride ($NaBH_4$) were purchased from Aldrich and used as received. The PVME ($M_v = 52\,000$) sample was a 50 wt % aqueous solution obtained from Aldrich. It was diluted to a 5 wt % solution with water and precipitated by heating to 70 °C. The precipitate was redissolved in water and precipitate again by heating. This process was repeated three times and finally dried in a vacuum oven for 2 days. The PSS ($M_w = 70\,000$) (Aldrich) and the NaCMC (British Drug House, London) samples were obtained in powdered form and were dissolved in a 0.01 M HCl to prepare a stock solution of 6 and 2 wt % respectively (pH 2.5). The viscosity-averaged molecular weight of NaCMC was determined to be 65 000.

Synthesis and Characterization of Poly (vinyl methyl ether)-Coated Gold Nanoparticles (PVME-GNPs). A 5 mL sample of 0.01 M $HAuCl_4$ solution was added to 5 mL of 5 wt % aqueous PVME solution, and the mixture was taken in a reaction vessel fitted with a temperature controller. The mixture was stirred for an hour at 20 °C, and to that 5 mL Milli-Q water was added. The $HAuCl_4$ was then reduced by dropwise addition of 5 mL of 0.01 M $NaBH_4$ solution with constant stirring and continued for 1 h that resulted in a development of wine-red color indicating the formation of GNPs. The mixture was further stirred for 24 h and then stored in the refrigerator. The GNPs were then centrifuged and washed three times to get rid of excess PVME and other impurities and finally redispersed in Milli-Q water to obtain a wine-red-colored suspension, which are stable at room temperature for a long period of time and was used in the assembly study.

UV−vis spectra of the PVME-GNPs suspensions were recorded on a Hewlett-Packard model 8453 Spectrophotometer equipped with a temperature-controlled multicell holder.

For transmission electron microscopy (TEM) studies a drop of the PVME-GNPs suspension was placed on a carbon-coated copper grid, and excess solution was removed by wicking using a filter paper. The grid was then dried in air and imaged on a JEOL JEM-200CX transmission electron microscope using an accelerating voltage of 120 kV. The size of the gold colloids was then determined by analysis of TEM image.

The amount of PVME adsorbed on the GNPs surface was determined by a thermogravimetric analyzer (TGA) using a Mettler Toledo Star System TGA/SDTA851e in the presence of N_2 gas with a heating rate of 20 °C/min.

LCST Study. The phase transition of pure PVME was determined in aqueous solution by monitoring the optical density at 490 nm as a function of temperature on a UV−vis spectrophotometer. The concentration of PVME was kept constant at 0.2 wt %, and that of PSS and NaCMC was varied. The pH of the assembly medium was same as that of the stock polyelectrolyte solutions (pH = 2.5).

Study of the Assembly of PVME-GNPs. The temperature-dependent assembly of PVME-GNPs in the presence of polyelectrolytes was monitored by measuring the SPR absorption of colloidal GNPs suspension as a function of temperature. The temperature was varied in steps of 2 °C over 20−40 °C. A thermometer was used to monitor the temperature of the solution in the cuvette. The absorption spectra were collected between 190 and 1100 nm, and the absorbance maximum between 500 and 600 nm was used as an indicator of assembly formation.

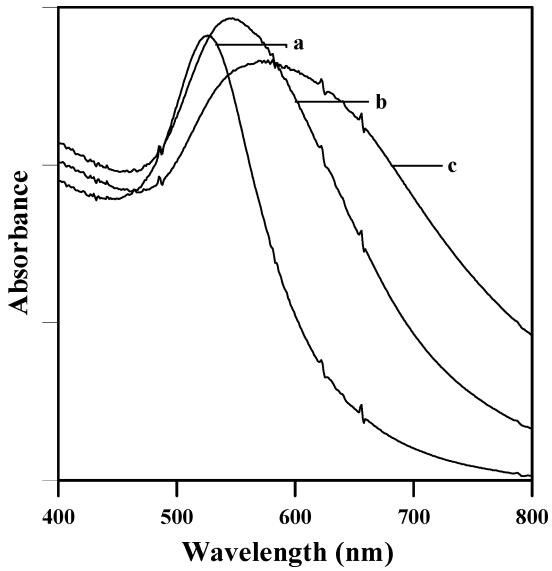

Figure 1. Effect of temperature on the UV−vis absorption spectra of centrifuged/redispersed PVME-GNPs suspension in absence of PSS at pH 2.5: (a) 20 °C; (b) 34 °C; (c) 36 °C.

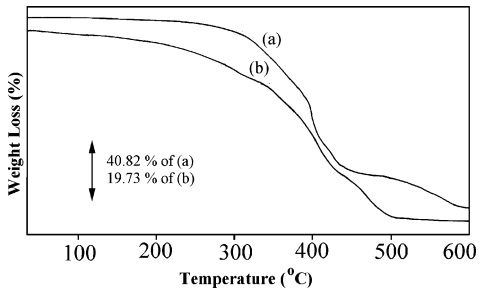

Figure 2. TGA thermograms of (a) neat PVME and (b) PVME-GNP composites.

The pH of the assembly medium measured to be 2.5, which was same as that of the polyelectrolyte solutions because the redispersed PVME-GNPs suspension was neutral. pH was increased from 2.5 to 10 by adding 0.1 M NaOH solution for reversibility study. In all the cases, we did not observe any "salting out" effect.

The morphology of the assembly of PVME-GNPs in the presence of PSS and NaCMC was studied by TEM. The samples for TEM study were taken out of the cuvette during the temperature-dependent UV−vis spectroscopic study and cast on a carbon-coated copper grid. The air-dried copper grid containing the self-assembled PVME-GNPs was then imaged at an accelerating voltage of 120 kV.

Results and Discussion

Preparation and Characterization of PVME-GNPs. The UV−vis spectrum of the centrifuged/redispersed PVME-GNPs suspension displays a surface plasmon resonance (SPR) band at 524 nm (Figure 1a), which did not change upon keeping the suspension for more than a month (see Figure S1 in the Supporting Information). TEM image of the PVME-GNPs revealed well-dispersed nanoparticles without any agglomeration, which will be discussed later in the morphology section. These results clearly indicate that the PVME-GNPs exhibit potential long-term stability. Figure 2 depicts the TGA curves of neat PVME and centrifuged/washed PVME-GNPs composites. According to the thermograms, pure PVME starts decomposing at ~300 °C, whereas the composite material is stable

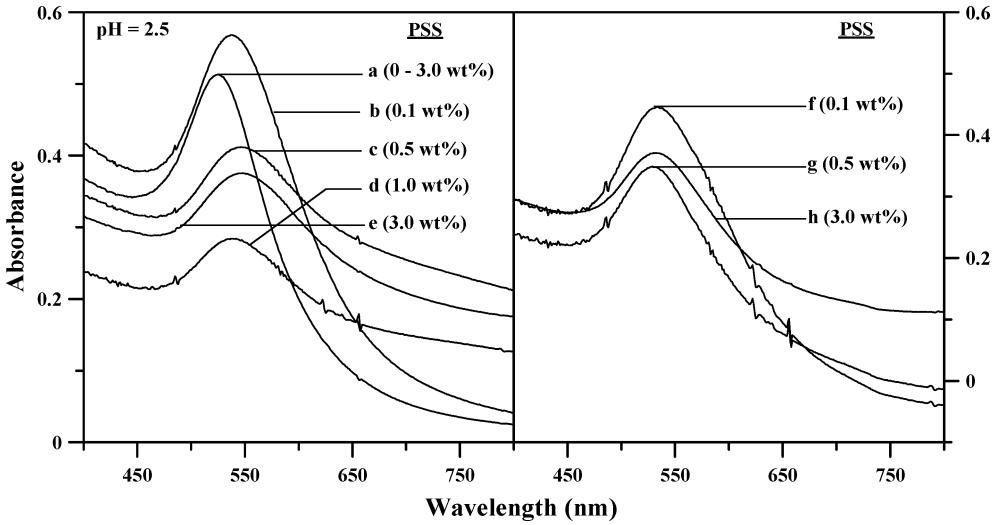

Figure 3. UV−vis spectra of PVME-GNPs suspensions in the presence of PSS at various temperatures: (a) 20; (b) 39; (c) 39; (d) 36; (e) 34 °C; (f)−(h) after cooling the mixture to 20 °C.

only up to ∼220 °C, which indicates that GNPs promote the decomposition of PVME. Earlier, Walker et al. have also observed similar type of lowering of decomposition temperature of poly(methylphenylphosphazene) upon adsorption on the surface of GNPs.[29] The reason for this could be the interaction between PVME and the GNPs that impart perturbation to the polymer structure and resulted in the weakening of the van der Waals forces between the polymer chains as mentioned by Kumar et al.[30] The binding of PVME to the surface of GNPs may have occurred through the interaction of the oxygen atoms of the pendent methoxy (−OMe) groups of PVME to the gold surface as in the case of poly(ethylene oxide) adsorption on GNP surface.[31] The significant weight loss, registered in case of pure PVME (Figure 2a) was 100% between ∼220 and 520 °C. However, for the composite in the same temperature range, the corresponding loss was only 44% (w/w), which is attributable to PVME assuming complete decomposition of the polymer, as the inorganic component remains thermally stable at that temperature range.[32]

Temperature-Dependent Assembly/Disassembly of PVME-GNPs in the Presence of PSS. The assembly of PVME-GNPs was monitored by the evaluation of SPR band of GNPs as a function of added PSS concentration and temperature cycled from 20 to 40 °C. The assembly process was visualized from the gradual color change of the Au sol from red to purple and ultimately to blue. All the measurements were performed at pH 2.5, where dissociation of sulfonic acid group of PSS is extremely restrained.[24,25] This was done to achieve effective interpolymer complexation between the added PSS and the PVME bound to GNP surface. In absence of PSS, the spectrum for PVME-GNPs suspension (Figure 1a) did not change as the solution temperature was increased to 55 °C (much above LCST of PVME ∼34 °C). This result indicates that the LCST of PVME has increased due to anchoring of PVME on Au nanoparticles surface, as evident from the TGA data shown in Figure 2b. We believe that the interaction of methoxy (−OMe) group of PVME with the GNP surface hinders the hydrophobic association of PVME chains, which results in increased hydrophilic character of the surface-bound PVME and results in a shift of LCST to higher temperature. However, at pH 2.5, the SPR band of PVME-GNPs red shifts from 524 to 547 nm at 34 °C along with a color change from red to blue and then shifted further to 575 nm at 36 °C (see parts b and c of Figure 1). We reason that, at low pH, the interaction of ethereal oxygen toward a proton is strong enough to weaken the Au−O interaction, which might result in weakening of the Au−O interaction. In fact, it has been reported in the literature that though the ethereal oxygen is weakly basic, still it can be effectively "protonated" at very low pH.[33] Thus, the interaction between −OMe group of PVME and GNP surface, which actually hinders the hydrophobic association of PVME chains, may not operate. As a result the surface-bound PVME can be easily associated through hydrophobic interaction near the LCST (34 °C) that leads aggregation of PVME-GNPs and the rate of aggregation increases as the temperature is increased from 34 to 36 °C.

Figure 3 displays a set of representative UV−vis spectra, recorded after the addition of PSS to the PVME-GNPs suspensions at 20 °C and the temperature at which the SPR band exhibited maximum red shift. The spectra of PVME-GNPs remained unchanged ($\lambda_{max} = 524$ nm) after the addition of PSS (0−3 wt %) as the temperature of the mixture was increased from 20 to 30 °C (Figure 3a). As the temperature was increased beyond 30 °C, the SPR band gradually changed with temperature depending on the concentration of PSS in the mixture. At 0.1 wt % PSS, the SPR band red shifted from 524 to 538 nm with peak broadening as the temperature was increased to 39 °C (Figure 3b). For 0.5 wt % PSS, the band shifted to 547 nm at 39 °C (Figure 3c). When the amount of PSS in the mixture was increased further to 1 wt %, a red shift of the SPR band from 524 to 539 nm was observed at 36 °C (Figure 3d). Further increasing the concentration of PSS to 3 wt % resulted in a red shift of 24 nm (524 to 546 nm) of the SPR band at 34 °C (Figure 3e). These observations substantiate that, below 0.5 wt % PSS, the SPR band of PVME-GNPs red shifted at temperatures much higher than LCST, whereas concentrations above 0.5 wt %, such red shifts were observed at temperatures close to LCST. The SPR band intensity of the assembled GNPs was observed to be substantially decreased for moderate (0.5 wt %) and high PSS concentrations (above 0.5 wt %) compared to that of low PSS concentration (0.1 wt %) at high temperature. The decrease in intensity may be due to multilayered or three-dimensional assembly of GNPs as suggested by Lazarides and Schatz.[34]

When the mixtures cooled back to 20 °C, the SPR absorption band of PVME-GNPs did not return exactly to 524 nm but blue shifted to 534, 529, and 525 nm for 0.1, 0.5, and 3 wt % PSS, respectively (see parts f, g, and h of Figure 3). However, the optical density of SPR bands was observed to be decrease for high PSS concentration after cooling. The reduced optical

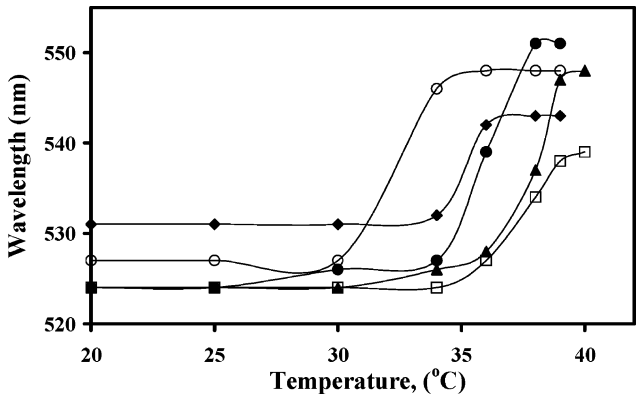

Figure 4. Plot showing the variation of SPR band position of PVME-GNPs suspensions with change in temperature in the presence of PSS of varying concentrations: (◆) 0.05; (□) 0.1; (▲) 0.5; (●) 1.0; (○) 3.0 wt % at pH = 2.5.

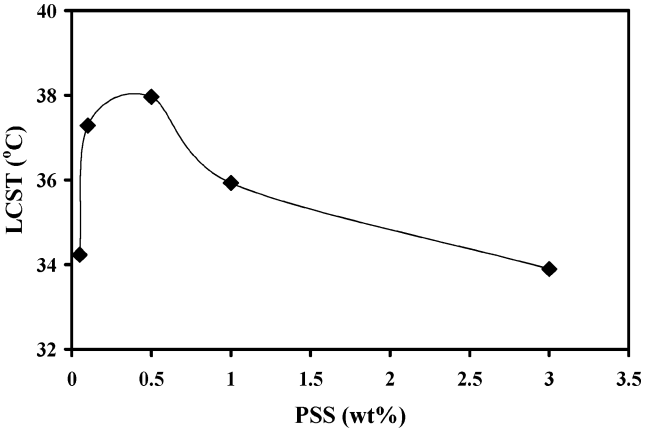

Figure 5. Plot showing the variation in slopes of the curves (i.e., LCST of surface bound PVME) in Figure 4 against concentrations of PSS.

density may be due to the decreased thermal stability of the PVME-GNPs at moderate and high PSS concentrations. The reason for the above thermoreversible spectral changes for PVME-GNPs may be due the hydrophobic effect of PSS that influences the LCST of the surface adsorbed PVME. Details have been discussed later in the mechanism section.

Effect of PSS on the LCST of PVME. To investigate the effect of PSS addition on the assembly of PVME-GNPs in more detail, the position of SPR band was plotted against temperature for particular PSS concentrations as shown in Figure 4. In each case, there is an abrupt change in position of SPR band at a particular temperature, which may actually correspond to the LCST of PVME, adsorbed on the gold surface. The measured LCST by this technique was then plotted against the concentration of PSS in the mixture (Figure 5). The data clearly shows that the LCST initially increases and reaches a maximum at about 0.5 wt % of PSS and then decreases as the concentration of PSS increases.

For comparison, LCST of aqueous solution of neat PVME has been measured in the presence and absence of PSS at pH = 2.5. The variation of light absorption at 490 nm of a 0.2 wt % aqueous pure PVME solution as well as in the presence of PSS of varying concentration was plotted as function of temperature (see Figure 6). The sudden jump in the absorbance value indicates the phase separation of PVME due to hydrophobic interactions of the side chain methyl groups.[22] The LCST was then determined from the slopes of the curves and was plotted against the concentrations of PSS as shown in inset of Figure 6. It also indicates that LCST of PVME initially increases

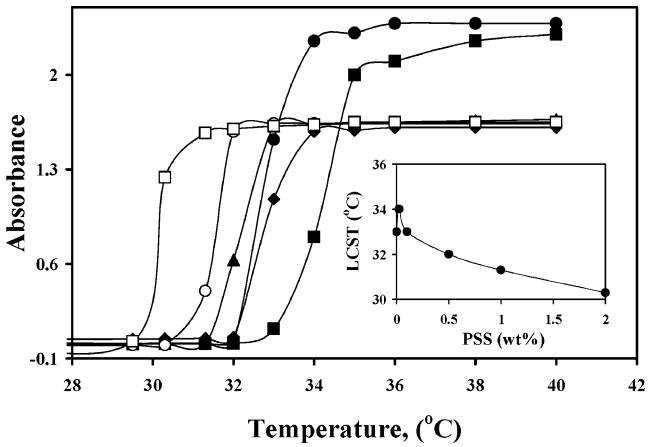

Figure 6. Variation of the light absorbance at 490 nm versus temperature for a neat PVME 0.2 wt % aqueous solution (◆) and of its mixtures with different PSS concentrations (■) 0.025, (●) 0.1, (▲) 0.5, (○) 1.0, and (□) 2.0 (%, w/v) at pH = 2.5. Inset shows the variation of LCST of pure PVME obtained from the slope these curves with PSS concentration.

and then decreases with the increase of PSS concentration. This result agrees well with the decreasing trend of LCST of surface adsorbed PVME, measured from the spectral change of PVME-GNPs as described above (Figure 5). Although, it has been reported in the literature that the LCST of PVME increases upon addition of polyacid such as PAA at moderate concentrations (0.3 wt %).[22] In our case, an initial increase in LCST of PVME is observed at moderate PSS concentrations (0.5 wt %) (Figure 5), which probably results from the increase of thermal stability of surface adsorbed PVME due to interpolymer complexation. But at high concentrations (above 0.5 wt %), there is increase in the hydrophobicity of the medium along with an increase in effective H^+ concentration due to high degree of dissociation of SO_3H group in PSS, compared to the COOH group in PAA,[35] which ultimately results in the decrease of stability of the IPC formed between surfaces adsorbed PVME and PSS.[22] Details have been discussed in the mechanism section.

Temperature-Dependent Assembly/Disassembly of PVME-GNPs in the Presence of NaCMC. Similarly, upon addition of NaCMC solution of varying concentration to PVME-GNPs suspensions, we studied the assembly of GNPs by monitoring the SPR band within the temperature span of 20−35 °C. Absorption measurements were conducted at pH 2.5 to minimize the ionization of carboxylic acid group of NaCMC, which favors H-bonding interaction between PVME and NaCMC chains. The spectrum of the PVME-GNPs in the presence of NaCMC (0.1%, w/v) displayed an absorbance maximum at 524 nm at 20 °C and is similar to the spectrum of uncomplexed PVME-GNPs (Figure 7a), which did not show any change up to 30 °C (Figure 7b). This SPR band at 524 nm was broadened and red shifted to 545 nm at 30 °C when the concentration of NaCMC was increased to 0.3 wt % (Figure 7c). At 0.7 wt % of NaCMC, the SPR band red shifted to 561 nm at 28 °C (Figure 7d).

The effect of cooling on the absorption spectra of PVME-GNPs suspension in the presence of NaCMC (0.3 wt %) was displayed in Supporting Information (see Figure S2). The SPR band maximum was observed to be blue shifted from 545 to 535 nm, when the temperature was lowered from 30 to 20 °C. The blue-shifted SPR band is almost similar to the band observed before heating, which indicates reversible assembly of the GNPs (see Supporting Information for details). From the thermodynamic point of view, lowering the temperature of a system disfavors any hydrophobic interactions. Hence, we can

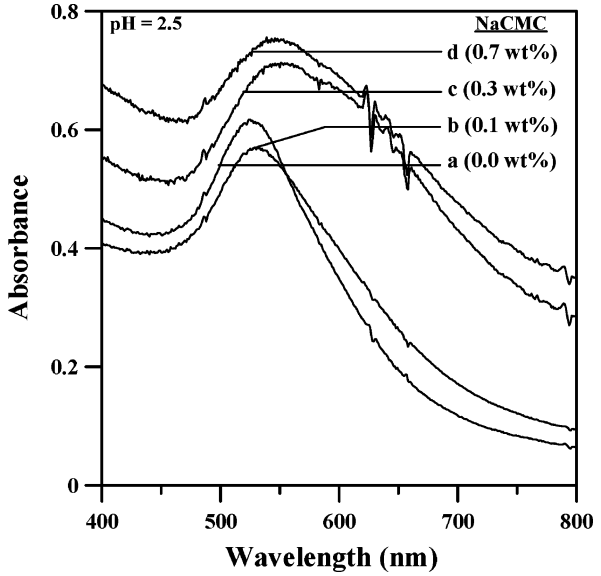

Figure 7. UV−vis spectra of PVME-GNPs suspensions in the presence of NaCMC at different temperatures: (a) 20; (b) 30; (c) 30; (d) 28 °C.

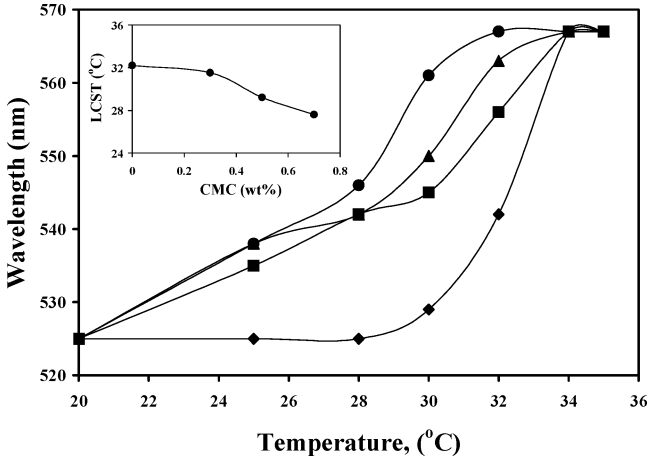

Figure 8. Plot showing the variation of SPR band position of PVME-GNPs with temperature at different NaCMC concentrations: (■) 0.3 wt %; (▲) 0.5 wt %; (●) 0.7 wt %; (◆) 0 wt %. Inset shows the plot depicting the variation in slopes (i.e., LCST of surface bound PVME) of these curves against the concentrations of NaCMC.

conclude that in the presence NaCMC, the interparticle hydrophobic interaction between the neighboring PVME-GNPs weakens upon lowering the temperature. This causes the dissociation of PVME-GNPs aggregates and returns the SPR maximum to 535 nm (Figure S2c). The extent of reversibility depends on the concentration of NaCMC and temperature.

Effect of NaCMC on the LCST of PVME. The maximum of the SPR bands were plotted against temperature for particular NaCMC concentrations, as in the case of PVME-GNPs and PSS system, and shown in Figure 8. As mentioned earlier, the LCST of surface adsorbed PVME is manifested through an abrupt change in the position of SPR band, which was plotted against the concentration of NaCMC as shown in the inset of Figure 8. In this case, we have also observed similar trend of decreasing LCST of adsorbed PVME on GNP surface with increasing NaCMC concentration as in the case of PVME-GNPs and PSS system.

We have also measured the LCST of neat aqueous PVME solution in the presence of varying concentration of NaCMC by similar turbid metric experiment as mentioned earlier for PSS at pH 2.5 (see Figure 9) for comparison. The measured

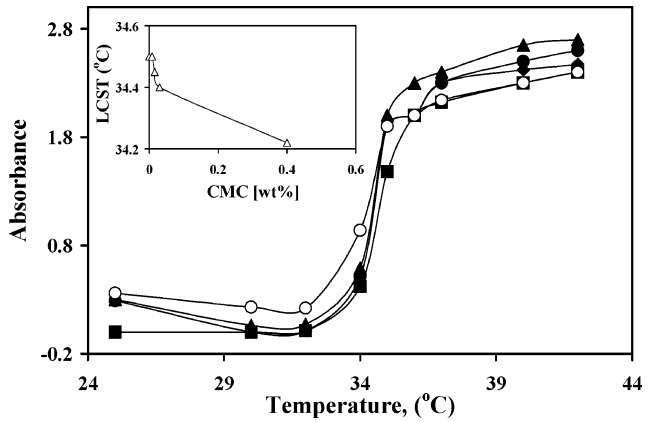

Figure 9. Variation of the light absorbance at 490 nm vs the temperature for a neat PVME 0.2 wt % aqueous solution (◆) and of its mixtures with different NaCMC concentrations: (●) 0.008; (▲) 0.016; (■) 0.03; (○) 0.4 (wt %, w/v) at pH = 2.5. Inset shows the variation of LCST of pure PVME solution obtained from the slope of these curves with NaCMC concentration.

TABLE 1: Values of λ_{Max} of SPR Band of PVME-GNPs during Their Assembly in Presence of a Particular Concentration of PSS and NaCMC at Different pH and Temperature (Corresponding Absorption Spectra Were Depicted in the Supporting Information)

polyelectrolytes	temperature (°C)	pH	λ_{max} (nm)
0.5 wt % PSS	20	2.5	524
	39	2.5	547
	39	10	529
0.3 wt % NaCMC	20	2.5	524
	30	2.5	545
	30	10	535

LCST was then plotted against concentration of NaCMC (see inset of Figure 9) and found that the result agrees quite well with the change of LCST of surface adsorbed PVME with NaCMC as measured form spectral change of PVME-GNPs (see Figure 8).

Effect of pH on the Assembly/Disassembly of PVME-GNPs in the Presence of PSS and NaCMC. The effect of pH on the assembly/disassembly of PVME-GNPs in the presence of these polyelectrolytes of particular concentration was summarized in Table 1 (for corresponding UV−vis spectra see Figure S3 and S4 in SI). The data in the table clearly indicates that at pH 2.5, the sharp SPR band at 524 nm was broadened and shifted to 547 nm due to the temperature triggered (20−39 °C) assembly of PVME-GNPs in the presence of 0.5 wt % PSS. The resultant SPR band (λ_{max} = 547 nm at 39 °C) was blue shifted to 529 nm upon increasing the pH of the medium from 2.5 to 10 and the band became sharp (see Figure S3 in SI). Such a blue shift of the SPR band of the PVME-GNPs indicated disassociation of colloidal aggregate might be due the breakage of interpolymer complex. In the case of NaCMC (0.3 wt %), we have observed similar kind of pH dependency, as the final SPR band of PVME-GNPs (λ_{max} = 545 nm at 39 °C) was blue shifted to 535 nm upon changing the pH from 2.5 to 10 (see Table 1). The pH-dependent assembly of PVME-GNPs was also studied with other PSS and NaCMC concentrations, and we observed similar spectral change as in the case of 0.5 wt % PSS and 0.3 wt % of NaCMC. Control experiments without adding any PSS shows that the color of the solution remained blue after pH was increased to 10 (see Figure S5 in SI). The broad band in Figure S5 indicated aggregated GNPs.

At neutral pH, it is expected that the adsorbed PVME on the gold surface have no H-bonding interaction with charged

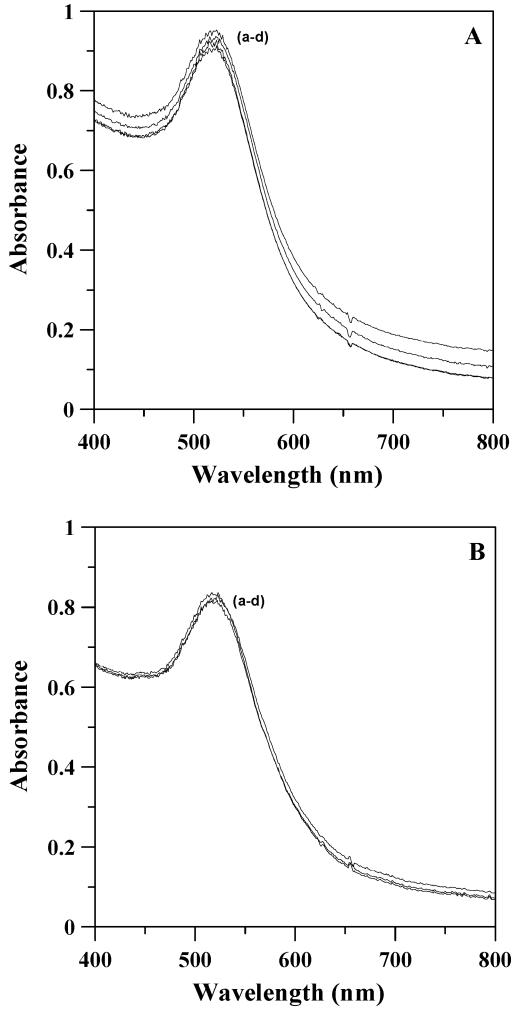

Figure 10. UV−vis spectra of PVME-GNPs suspension in the presence of (A) 0.5 wt % PSS at various temperatures (a−d) overlaid spectra at 25, 30, 35, and 40 °C and (B) 0.7 wt % CMC at various temperatures (a−d) overlaid spectra at 25, 30, 35, and 40 °C at neutral pH.

polyelectrolytes (PSS and NaCMC) because of the dissociation of the carboxylic and sulfonic acid groups and hence there will be no spectral change of PVME-GNPs at this pH. To confirm this issue, we have monitored the spectral behavior of PVME-GNPs in the presence of polyelectrolytes at neutral pH. But we did not observe any change in SPR properties of the PVME-GNPs in the presence of varying concentrations of PSS and NaCMC at temperature up to 40 °C as shown in Figure 10. These results strongly suggest that the polyelectrolytes do not form interpolymer complex through H-bonding with PVME adsorbed on the gold surface at neutral pH.

Morphology Study. Parts a and b of Figure 11 display the TEM micrographs of the as-prepared and the centrifuged/redispersed PVME-GNPs, respectively. It is evident from the images that the nanoparticles are well dispersed after removal of excess PVME from the GNP surface. The average particle size of the as-prepared PVME-coated GNPs was found to be 7.7 ± 1.5 nm as estimated from the statistical analyses of TEM images (see Figure S6 in SI for histogram analysis). Parts c and d of Figure 11 display the TEM micrographs of the assembled PVME-GNPs in the presence of 0.1 and 1 wt % of PSS and the samples were taken at 39 and 36 °C, respectively. Networklike architectures of GNPs (Figure 11c) were observed in the presence of 0.1 wt % PSS. However, at higher PSS concentration (1 wt %), GNPs were assembled into three-dimensional structures (Figure 11d). UV−vis spectra of both the samples were different (parts b and d of Figure 3, respectively), which indicate that the mode of assembly is different for lower and higher PSS concentrations. The TEM micrograph of the PVME-GNPs in the presence of 0.4 wt % NaCMC at 30 °C (Figure 12) show mostly ordered two-dimensional assembly of GNPs with a few three-dimensional features at some places. The rate of assembly in case of NaCMC can be controlled by varying the concentration of the polyelectrolyte, temperature, and addition of methanol to the GNPs sol prior to the addition of NaCMC solution. Methanol increases the stability of PVME, and it is also an effective hydrophobicity destructor.[36] We are presently working on the controlled assembly of PVME-GNPs under different conditions.

Control Experiments. We have performed some control experiments using a nonthermoresponsive analogue of PVME such as citrate-stabilized GNPs in the presence and absence of polyelectrolytes at pH 2.5. These results show no change in the SPR properties of citrate-capped GNPs. Furthermore, it is well-known that both the polyelectrolytes (PSS and NaCMC) have no thermoresponsive behavior. Thus, we can conclude that the PVME-GNPs only display temperature-dependent SPR properties in the presence or absence of polyelectrolytes.

To check whether there is any possibility of displacement of PVME from the GNPs surface by PSS or NaCMC at pH 2.5 through the ligand exchange reaction, we have monitored the SPR band position of PVME-GNPs in the presence of these polyelectrolytes of varying concentration at 20 °C and did not observe any change in SPR properties colloidal PVME-GNPs suspensions (see Figure 3a). The SPR peak of GNPs usually changes when the surface adsorbed ligands are exchanged with some other ligands. For example, the SPR peak corresponds to citrate-stabilized GNPs has been shifted from 519 to 524 nm during the exchange of ligand with thiol-functionalized DNA.[37] Very recently, Caruso et al. have been reported that the plasmon band of the 4-(dimethylamino) pyridine-GNPs in solution red shifts and broadens in the presence of PSS.[38] Thus, we believe that no exchange reaction is taking place between the PVME adsorbed on the gold surface and the polyelectrolytes in solution.

Mechanism of Assembly/Disassembly of PVME-GNPs. The temperature-dependent self-assembly of PVME-GNPs in the presence of polyelectrolytes can be explained from the scheme as shown in Figure 13. In presence of PSS and at low pH, the H atoms of the SO_3H participate in cooperative hydrogen bonding with the ether oxygen atoms of the surface bound PVME of PVME-GNPs (species **1**) to form an interpolymer complex resulting in a energetically favorable species **2**, which partially dissociates to species **3**.[22] There might be some hydrophobic interactions between the pendant methyl groups of PVME on GNP surface and the phenyl groups of PSS that also increases the stability of the interpolymer complex (species **2**). In this case, the number of free H^+ ions available for complexation of the −OMe group of surface-bound PVME is actually very small compared to that of the PVME-GNPs composite without PSS at the same H^+ ion concentration. The majority of H^+ ions in solution are consumed by the PSS to protonate the SO_3^- group of PSS. Because of the less available H^+ ions, the O−Au bond is less labile and so the surface bound PVME mainly remains hydrophilic.

At low PSS concentration and 20 °C, the negative charge on the surface of species **3** imparts extra thermal stability to the colloidal PVME-GNPs, and hence it is stable above the LCST of adsorbed PVME. With increase in temperature, the cooperative hydrogen bonds start to break and the interpolymer complex (IPC) (species **3**) slowly disintegrates into partially disintegrated

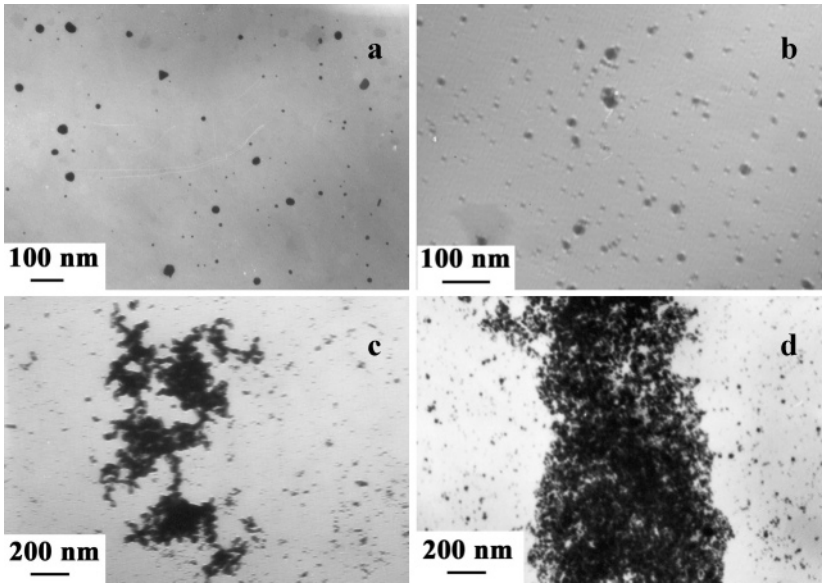

Figure 11. TEM images of PVME-GNPs: (a) as-prepared; (b) centrifuged/redispersed; (c) assembled in the presence of 0.1 wt % PSS; (d) assembled in the presence of 1 wt % PSS.

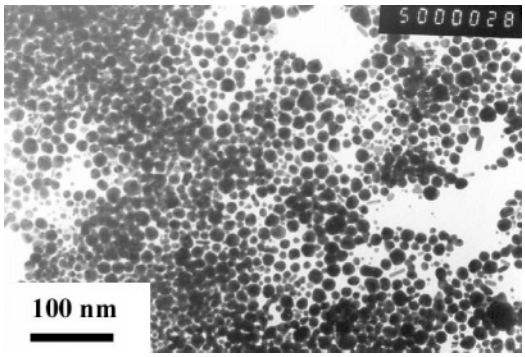

Figure 12. TEM image of assembled PVME-GNPs in the presence of 0.4 wt % NaCMC at 30 °C.

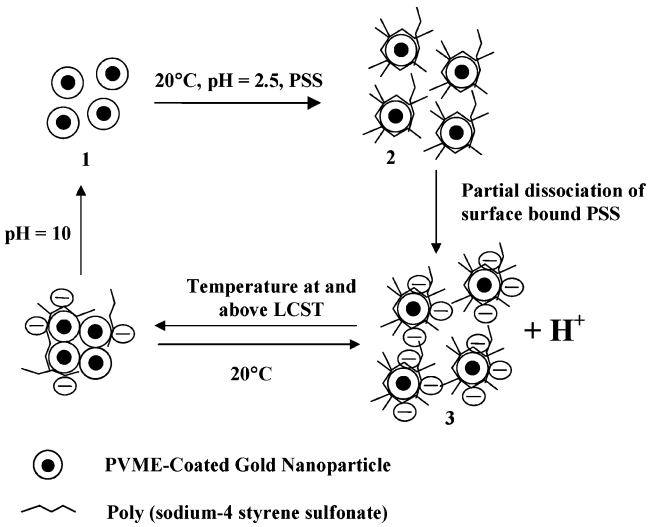

Figure 13. Schematic representation of possible mechanism of the assembly/disassembly of PVME-GNPs in the presence of polyelectrolytes due to interpolymer complex formation.

species **1**, which results in the formation of controlled assembly of the PVME-GNPs (Figure 11c) due to the hydrophobic association of surface adsorbed PVME chains. When PSS concentration is increased (above 0.5%), the interpolymer complex between surface bound PVME and PSS also become more compact[22] due to the increase in the number of hydrophobic phenyl groups of PSS. The more compact structure of the species **2** results in the shrinkage of the PVME chain that favors the formation of hydrophobic clusters through the aggregation of the side-chain methyl groups[22] and decrease the stability of the PVME-GNPs. Also due to high dissociation constant of SO_3H, the effective H^+ concentration increases, which increase the concentration of less soluble species **2**.[22] This may be the reason for assembly of PVME-GNPs at temperatures closer to LCST (e.g., at 36 °C for 1% PSS) with increasing PSS concentrations. During the cooling process, hydrogen bonds are regenerated and the hydrophobic effect becomes thermodynamically less favorable so that the association between the surface adsorbed PVME chains on different GNPs decrease. This results in the formation of partially disintegrated species **3** showing thermo reversibility of the assembled GNPs (parts f, g, and h of Figure 3).

The mechanism of the assembly of PVME-GNPs in the presence of NaCMC is a little different compared to that of PSS. At pH 2.5, the carboxylate group of the NaCMC side chain converts to carboxylic acid and forms hydrogen bonds with the oxygen atoms of the pendent ether groups of PVME, simultaneously exposing the hydrophobic methyl groups in solution. The stability of PVME against association in aqueous solution depends largely on the hydrophobic hydration of the above-mentioned methyl groups. Due to the presence of β-glucose-like structure in the main chain of NaCMC, it is expected that CMC chains will induce competitive hydrophobic hydration[39,40] in aqueous medium and hence decrease the hydrophobic hydration sheath of the surface bound PVME. The exposed methyl group of surface-adsorbed PVME form hydrophobic clusters[22] that result in the assembly of the GNPs at room temperature and above. Hence, the temperature, at which the hydrophobic clustering of the GNPs occurs, is actually the manifestation of the LCST of surface bound PVME. When the NaCMC concentration is increased, the GNPs assemble at temperatures below LCST due to an effective increase in the extent of hydrophobic clustering (Figure 7). In case of bulk PVME, the lowering of the LCST in the presence of NaCMC at low pH (Figure 9) is less pronounced compared to that of the surface bound PVME (Figure 8). On cooling, the hydrophobic clustering breaks down, which dissociates the colloidal GNP aggregates into dispersed nanoparticles and results in blue

shift of the surface plasmon resonance (SPR) band (Figure S2c). Thus, we can conclude that the change of SPR properties due to the assembly of the PVME-GNPs in the presence of NaCMC at low pH give a better measurement of the change LCST of surface bound PVME in the presence of polyelectrolyte.

Conclusion

In conclusion, we have shown from the UV−vis spectral and TEM studies that PVME-GNPs have been self-assembled into three-dimensional structures in the presence of aqueous polyelectrolyte. This assembly process is reversible with respect to temperature and pH of the medium. The mechanism of assembly formation with PSS was different from NaCMC due to the difference in the nature of the two polyelctrolytes. But, the study with NaCMC established that temperature-dependent hydrophobic association/disassociation of the PVME chain adsorbed on the nanoparticle surface is the main driving force for this reversible assembly. The change in optical property due to this aggregation/disaggregation of GNPs enables us to use it as a tool to monitor the change LCST of PVME in the presence of polyelectrolytes due to interpolymer complexation at low pH. This result agrees well with the variation LCST of aqueous solution of pure PVME solution in the presence of polyelectrolytes measured by conventional turbidimetric technique.

Acknowledgment. Thanks to the Nanoscience and Nanotechnology Initiatives, DST, New Delhi for partial support of this research work. Thanks are also due to the partial support from the Department of Biotechnology, New Delhi.

Supporting Information Available: Colloidal stability study of PVME-GNPs at pH 2.5, effect of cooling on the SPR property of PVME-GNPs in the presence of NaCMC, UV−vis spectra of PVME-GNPs suspensions at different pH, and histogram analysis of Au nanoparticle sizes. This material is available free of charge via the Internet at http://pubs.acs.org.

References and Notes

(1) Mirkin, C. A.; Letsinger, R. L.; Mucic, R. C.; Storhoff, J. J. *Nature* **1996**, *382*, 607.
(2) Brown, S. *Nano Lett.* **2001**, *1*, 391.
(3) Cobbe, S.; Connolly, S.; Ryan, D.; Nagle, L.; Eritja, R.; Fitzmaurice, D. *J. Phys. Chem. B* **2003**, *107*, 470.
(4) Shenton, W.; Davis, S. A.; Mann, S. *Adv. Mater.* **1999**, *11*, 449.
(5) Mayya, K. S.; Schoeler, B.; Caruso, F. *Adv. Funct. Mater.* **2003**, *13*, 183.
(6) Chen, S.; Pei, R.; Zhao, T.; Dyer, D. J. *J. Phys. Chem. B* **2002**, *106*, 1903.
(7) Han, L.; Luo, J.; Kariuki, N. N.; Maye, M. M.; Jones, V. W.; Zhong, C. J. *Chem. Mater.* **2003**, *15*, 29.
(8) Boal, A. K.; Ilhan, F.; DeRouchey, J. E.; Thurn-Albrecht, T.; Russell, T. P.; Rotello, V. M. *Nature* **2000**, *404*, 746.
(9) Brown, J. J.; Porter, J. A.; Daghlian, C. P.; Gibson, U. J. *Langmuir* **2001**, *17*, 7966.
(10) Chen, S. *Adv. Mater.* **2000**, *12*, 186.
(11) Brust, M.; Bethell, D.; Schiffrin, D. J.; Kiely, C. J. *Adv. Mater.* **1995**, *7*, 795.
(12) Frankamp, B. L.; Uzun, O.; Ilhan, F.; Boal, A. K.; Rotello, V. M. *J. Am. Chem. Soc.* **2002**, *124*, 892.
(13) Kim, Y. J.; Johnson, R. C.; Hupp, J. T. *Nano Lett.* **2001**, *1*, 165.
(14) Xu, L.; Guo, Y.; Xie, R.; Zhuang, J.; Yang, W.; Li, T. *Nanotechnology* **2002**, *13*, 725.
(15) Schild, H. G. *Prog. Polym. Sci.* **1992**, *17*, 163.
(16) Bae, Y. H.; Okano, T.; Hsu, R.; Kim, S. W. *Macromol. Chem. Rapid Commun.* **1987**, *8*, 481.
(17) Feil, H.; Bae, Y. H.; Feijen, J.; Kim, S. W. *J. Membr. Sci.* **1991**, *64*, 283.
(18) Groehn, F.; Bauer, B. J.; Akpalu, Y. A.; Jackson, C. L.; Amis, E. J. *Macromolecules* **2000**, *33*, 6042.
(19) Chechik, V.; Crooks, R. M. *Langmuir* **1999**, *15*, 6364.
(20) Wuelfing, W. P.; Gross, S. M.; Miles, D. T.; Murray, R. W. *J. Am. Chem. Soc.* **1998**, *120*, 12696.
(21) Bhattacharjee, R. R.; Chakraborty, M.; Mandal, T. K. *J. Nanosci. Nanotech.* **2004**, *4*, 844.
(22) Karayanni, K.; Staikos, G. *Eur. Polym. J.* **2000**, *36*, 2645.
(23) Horne, R. A.; Almeida, J. P.; Day, A. F.; Yu, N. T. *J. Colloid Interface Sci.* **1971**, *35*, 77.
(24) Becturov, E. A.; Bimendina, L. A. *Adv. Polym. Sci.* **1981**, *41*, 99.
(25) Tsuchida, E.; Abe, K. *Adv. Polym. Sci.* **1981**, *45*, 1.
(26) Hemker, D. J.; Garza, V.; Frank, C. W. *Macromolecules* **1990**, *23*, 4411.
(27) Bokias, G.; Staikos, G.; Iliopoulos, I.; Audebert, R. *Macromolecules* **1994**, *27*, 427.
(28) Ohno, H.; Matsuda, H.; Tsuchida, E. *Macromol. Chem.* **1981**, *182*, 2267.
(29) Walker, C. H.; St. John, J. V.; Wisian-Neilson, P. *J. Am. Chem. Soc.* **2001**, *123*, 3846.
(30) Kumar, R. V.; Koltypin, Y.; Cohen, Y. S.; Cohen, Y.; Aurbach, D.; Palchik, O.; Felner, I.; Gedanken, A. *J. Mater. Chem.* **2000**, *10*, 1125.
(31) Longenberger, L.; Mills, G. *J. Phys. Chem.* **1995**, *99*, 475.
(32) Si, S.; Kotal, A.; Mandal, T. K.; Giri, S.; Nakamura, H.; Kohara, T. *Chem. Mater.* **2004**, *16*, 3489.
(33) Warshawsky, A.; Kalir, R.; Deshe, A.; Berkovitz, H.; Patchornik, A. *J. Am. Chem. Soc.* **1979**, *101*, 4249.
(34) Lazarides, A. A.; Schatz, G. C. *J. Phys. Chem. B* **2000**, *104*, 460.
(35) Iliopoulos, I.; Audebert, R. *Macromolecules* **1991**, *24*, 2566.
(36) Ikawa, T.; Abe, K.; Honda, K.; Tsuchida, E. *J. Polym. Sci., Polym. Chem. Ed.* **1975**, *13*, 1505.
(37) Storhoff, J. J.; Elghanian, R.; Mucic, R. C.; Mirkin, C. A.; Letsinger, R. L. *J. Am. Chem. Soc.* **1998**, *120*, 1959.
(38) Cho, J.; Caruso, F. *Chem. Mater.* **2005**, *17*, 4547.
(39) Kim, Y. H.; Kwon, I. C.; Bae, Y. H.; Kim, S. W. *Macromolecules* **1995**, *28*, 939.
(40) Lee, S. B.; Sohn, Y. S.; Song, S. C. *Bull. Korean Chem. Soc.* **2003**, *24*, 901.